To synthesize the three-arc trajectory, draw a unity circle C_1 tangent to both C_o and C_f as in Fig. 8b. The center of C_1 is the intersection of two arcs which are two radii from C_o and C_f, respectively. By using different combinations of initial and final circles in this construction, up to eight such centers can be found. At most, two of these can be used to draw circles that form confluent three-arc trajectories and that contain angles of more than π radians. The shortest of these two is another feasible optimum trajectory.

To construct the four-arc trajectory, denote by P_m the midpoint of the line connecting the center of the circles C_o and C_f. Draw a unity circle C_1 tangent to C_o with center at the intersection of two arcs, the first arc being two radii from C_o and the second arc one radius from P_m, as illustrated in Fig. 8c. Similarly, draw a second circle C_2 tangent to both the final circle C_f and the circle C_1. This procedure guarantees that the two-interior arcs of the four-arc trajectory are of equal length. At most, two four-arc trajectories with interior arcs containing angles of more than π radians can be drawn by using different combinations of initial and final circles.

This concludes the construction of all feasible optimum trajectories. The globally optimum trajectory can now be determined by comparing the length of all feasible optimum trajectories, and choosing the one with the shortest arc length.

References

[1] Miele, A., "Theory of Flight Paths," *Flight Mechanics*, Vol. 1, Addison-Wesley, Reading, Mass., 1962, Chaps. 4 and 9.

[2] Petrie, D. M., "Automatic Flight Management of Future High-Performance Aircraft," *Journal of Aircraft*, Vol. 5, No. 4, July–Aug. 1968, pp. 335–343.

[3] MacKinnon, D., "Quasi-Optimization of a Localizer Acquisition System," *Proceedings of the 1969 Joint Automatic Control Conference*, American Institute of Chemical Engineers, 1969, pp. 822–830.

[4] Athans, M. and Falb, P. L., *Optimal Control*, McGraw Hill, New York, 1966, Chaps. 5 and 6.

[5] Johnson, C. D., "Singular Solutions in Problems of Optimal Control," in *Advances in Control Systems*, Vol. 2, edited by C. T. Leondes, Academic Press, N. Y., 1965, pp. 209–267.

FEBRUARY 1971 J. AIRCRAFT VOL. 8, NO. 2

Boundary-Layer Discontinuity on a Helicopter Rotor Blade in Hovering

HENRY R. VELKOFF,* DWIGHT A. BLASER,† AND KENNETH M. JONES‡

The Ohio State University, Columbus, Ohio

An experimental study was conducted using flow visualization techniques to investigate the nature of the boundary layer on a model helicopter rotor. Hovering and forward flight data were obtained; however, efforts were concentrated on hovering when unanticipated boundary-layer behavior was revealed. The primary flow visualization technique involved the use of ammonia injected into the boundary layer at the leading edge. The blade surface was chemically coated, and as the ammonia moved with the local airflow, it formed a trace on the surface indicative of the boundary-layer flow. The hovering traces initially moved chordwise along the surface, and then abruptly turned outward. A short distance later, the traces moved inward and then continued aft along the blade in a somewhat diffuse pattern. Similar traces were found over wide ranges of pitch angles and rotor speeds. It is hypothesized that a standing laminar separation bubble exists on the blade surface aft of the peak pressure position. No indication of any separation bubbles could be found on the forward flight traces.

Nomenclature

c = blade chord length
L_1 = separation point
L_2 = reattachment point
P = pressure coefficient
ΔP = differential pressure
q = dynamic pressure, $\rho V^2/2$
r = radius to local blade section
R = blade radius
s_1 = stagnation point preceding the separation bubble
s_2 = stagnation point following the separation bubble
V = flight speed
V_r = resultant potential flow velocity at radius r
x = distance along midchord measured from the blade leading edge
θ = blade pitch angle
μ = advance ratio
ψ = azimuth angle
Ω = rotational speed of rotor

Presented as Paper 69-197 at the AIAA/AHS VTOL Research Design, and Operations Meeting, Atlanta, Ga., February 17–19, 1969; submitted January 26, 1970; revision received June 17, 1970. This work was sponsored under a contract with the U.S. Army Aviation Materiel Laboratories, "AVLABS" Fort Eustis, Va.

* Professor of Mechanical Engineering.

† Graduate student.

‡ Graduate student; now Associate Research Engineer, SST Division, The Boeing Company, Seattle, Wash.

Introduction

A FUNDAMENTAL limitation on the performance and utility of the helicopter is related to the onset of "stall" on the retreating blades. This stall limits the performance of the helicopter because of increased power requirements, increased aircraft roughness, vibration, and control loads. Blade stall, however, depends upon the nature of the boundary layer which exists on an airfoil. Relatively little information on the nature of the boundary layers on rotor blades has existed until quite recently.[1–4] The complexity of the rotor blade motion, the flowfield, and the fluid mechanic equations involved have tended to discourage research into the nature of the rotor blade boundary layers. It was the purpose of

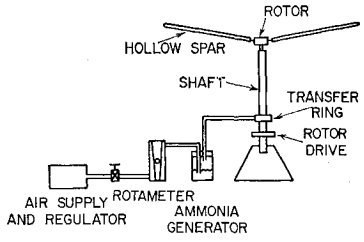

Fig. 1 Ammonia feed apparatus and rotor stand.

the investigation reported herein to initiate study into the physical nature of these boundary layers.

The scope of the action which may occur in rotor boundary layers is quite broad. The primary action is the chordwise viscous flow in the presence of the given chordwise pressure distribution. Flow components exist in both the chordwise and spanwise directions. The magnitude and direction of the local velocity varies around the azimuth and along the blade span as do the spanwise pressure gradients which exist.[6] Tip vortex induced flows exist which produce preceding blade wake interference.[7] The fluid particles within the boundary layer can experience centrifugal and coriolis effects. Compressible flow effects can occur on the tip of the advancing blade, reversed flow can occur in the inboard regions of the retreating blade, and very rapid angle of attack changes occur.[6] Periodic stall flutter and high rates of change of angle-of-attack effects on retreating blades have also been subject to intensive study.[4]

From the foregoing enumeration it is apparent that many interactions do indeed exist, and that detailed studies of rotor boundary layers should prove to be a fruitful field of research. Greater understanding of the boundary-layer actions would aid those efforts being made to produce better airfoils for helicopters, or those programs which seek to use boundary-layer control or jet flap devices to increase rotor performance.

Boundary-Layer Flow Visualization

Many processes used for flow visualization are not fully satisfactory for use in centrifugal fields because their density, quite different from that of air, causes them to experience outward force. Wool tufts, some chemicals, smoke, and oil are common visualization devices, but may be unreliable under these conditions since they may tend to average out potentially important actions in the boundary layer or may be susceptible to the high g fields. Subliming chemicals, such as acenaphthene, are useful for locating transition lines.

It was decided to search for a chemical trace technique which might overcome some of the limitations of the various probe methods or the subliming chemicals. The basic concept involved the injection of a tracer gas into the boundary layer which would react with a chemically coated surface of the rotor blade airfoil. After investigation of several chemical coatings, it was decided to use the ordinary blueline or "Ozalid" blueprint paper. Ammonia vapor was used as a reactant by injecting it through small orifices in the airfoil surface. Literature review revealed that the "Ozalid" or ammonia-azo method of flow visualization had been first used by Ruden in 1937 and more recently in 1964 by Johnson in the study of centrifugal compressors.[9]

To provide a reference between data taken in this study and that from other investigations, chemical sublimation tests were also conducted. This technique involved the application of acenaphthene dissolved in acetone to the airfoil surface.

Model Rotor Blades

The initial rotor tests with the ammonia trace technique were conducted using a two-bladed teetering model rotor mounted on a hover stand. The rotor utilized an NACA 0015 blade section with zero twist, 4-in. chord, and 6-ft diam. A leading edge orifice was located in one of the blades at 72% radius. Following initial tests with this rotor, additional orifices were added at the leading edge.

To provide for a wider range of Reynolds number, and as a check on the results with the 4-in. chord blade, tests were also conducted with a second rotor. This rotor used a single untwisted blade with an NACA 0015 airfoil, 7-in. chord, and 3-ft radius. Three orifices were located at the leading edge at positions of 61.5, 74, and 87% radius.

A third rotor was also used on the hover stand. This rotor used two blades identical to the 7-in. chord blade. Orifices were located on one of these blades at several chordwise and spanwise positions to obtain a complete network of traces.

Figure 1 illustrates the hover test stand including the ammonia generation system. The mixture of ammonia and air was directed to the transfer ring at the base of the rotor stand drive shaft, passed up through the hollow drive shaft and out a lateral port at the top of the shaft. It then flowed into the hollow blade spar and out of the orifices. The "Ozalid" paper was taped to the blade surface and pricked at each orifice to allow the ammonia to enter the boundary layer.

Test Results for 4-in. Chord Blade

The hover tests with the 4-in. chord blades and the orifice at 72% radius provided some extremely fascinating results. Consequently, specific emphasis is placed upon the findings with the 4-in. chord blades and upon the interpretation of these results.

Chemical Sublimation

All sublimation tests were conducted at 400 rpm, which provide a tip Reynolds number of 2.62×10^4. The pitch angle θ was varied from $-15°$ to $20°$. Previous sublimation tests were conducted by Tanner and Yaggy[10] at a Reynolds number of 1.1×10^6. In spite of the large difference in Reynolds numbers, the correlation between present results and Tanner's is very close for high pitch angles, as shown in Fig. 2. For pitch angles less than 8°, there is a greater difference, but the trends of the data are similar. The correlation of the data suggests that the location of transition may depend on the pitch angle more than the Reynolds number. Included in the figure is a curve from prior studies of transition for two-dimensional symmetrical airfoils based upon interpolation of the data presented.[11] The Reynolds number of those tests was 1.7×10^6. As expected the transition at the lower Reynolds number for the model rotor occurs farther aft on the chord. It can be seen that reasonably good correlation of the transition has been achieved even though a significant difference in Reynolds number exists.

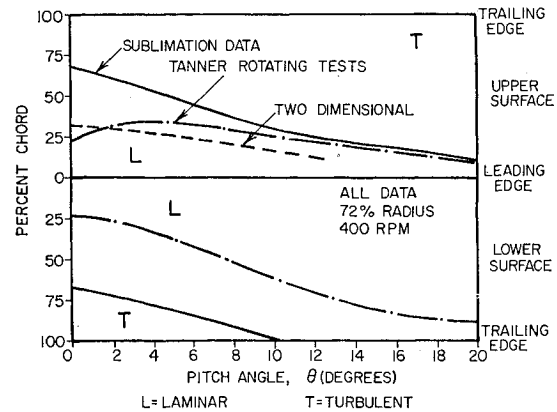

Fig. 2 Location of transition at 72% radius vs pitch angle from sublimation tests.

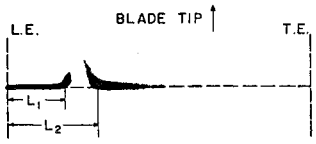

Fig. 3 Ammonia trace showing discontinuity for the 4-in. chord blade at 72% radius: L_1 = 13.5%, L_2 = 30% chord, 400 rpm, θ = 10°.

Ammonia Trace

Single orifice

When the ammonia was released from the leading edge, the resulting traces often showed a severe discontinuity. This can be seen in Fig. 3 for a pitch angle of 10° and a rotational speed of 400 rpm. Other examples of traces at 72% radius showing this discontinuity can be seen in Figs. 4 and 5. In an attempt to correlate and interpret this unusual trace behavior, the start of a discontinuity was located at the chord length where the flow first deviated from a straight chord line and designated by L_1. Similarly, the end of the discontinuity was placed at that point where the flow completely returned to the same straight chord line and designated as L_2.

Examination of Figs. 4 and 5 reveals a trend for discontinuities to be located farther back on the chord with slower speed. However, the differences involved between 300 rpm and 200 rpm were generally under 3% of the chord. The discontinuity is more strongly influenced by changes in the pitch angle. As can be observed from Fig. 4 or 5, the discontinuities are nearer the leading edge and shorter for increased pitch angle.

Figure 6 contains data from both the ammonia traces and the sublimation tests for various pitch angles. There is strong correlation between the end of the discontinuity and the point of transition.

The chordwise pressure distribution is an important factor in determining the location of boundary-layer transition. Since the end of an ammonia trace discontinuity corresponds closely with the point of transition, the start of a discontinuity was examined for correlation with the chordwise pressure distribution. The correlation used is based upon the chord at which the pressure is 90% of its maximum value and the results are also plotted in Fig. 6. Correlation is quite good for pitch angles less than 10°. At higher angles the start of a discontinuity lags behind the 90% pressure location.

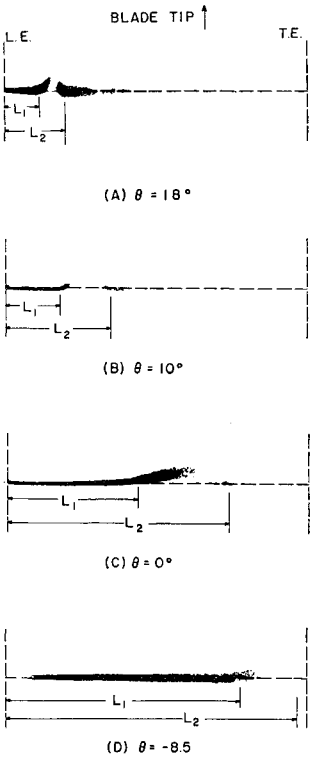

Fig. 4 Traces for 4-in. chord blade, 72% radius at 300 rpm and various values of θ: A) L_1 = 8%, L_2 = 16.5%; B) L_1 = 15%, L_2 = 32%; C) L_1 = 39%, L_2 = 79%; D) L_1 = 76% L_2 = 97%.

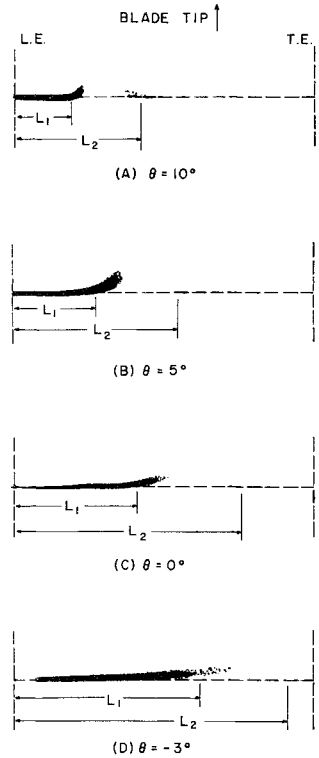

Fig. 5 Traces for 4-in. chord blade, 72% radius at 200 rpm and various values of θ: A) L_1 = 15.5%, L_2 = 38%; B) L_1 = 22%, L_2 = 50%; C) L_1 = 36%, L_2 = 74%; D) L_1 = 66%, L_2 = 91%.

Multiorifice

To determine the boundary-layer flow in hovering at various positions along the blade, tests were conducted with the 4-in. chord blade with 8 leading edge orifices located at increments of 10% radius. Typical results are shown in Fig. 7. This figure presents data for a rotor speed of 400 rpm and five pitch angles.

By examining the spanwise set of traces at a given pitch angle it can be seen that a fairly regular change in the discontinuity exists from inboard to outboard region. The discontinuity is generally wider and farther aft in the inboard region of the blade. The dashed line represents the location

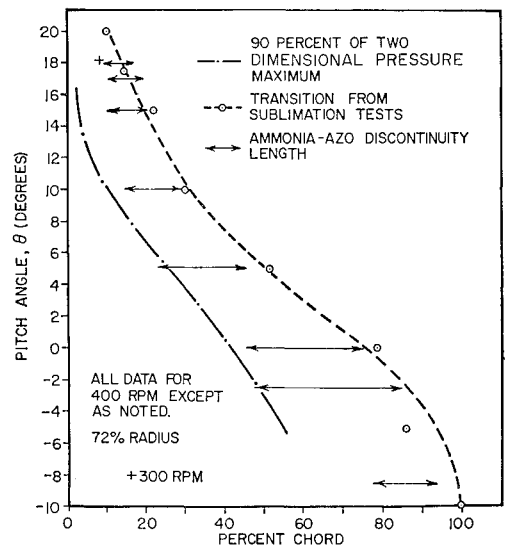

Fig. 6 Comparison of ammonia-azo discontinuity and transition point for various pitch angles.

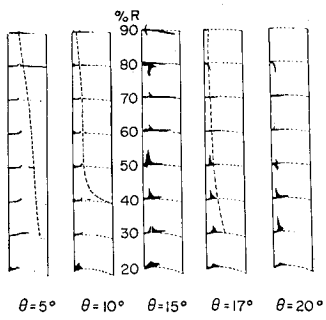

Fig. 7 Traces at several radii for the 4-in. chord blade at various pitch angles and 400 rpm.

of transition obtained from the sublimation tests. In most instances transition occurs just aft of the discontinuity as had been indicated by the comprehensive tests at 72% radius.

The changes in the pattern with radius can be the result of two separate actions. First, the tangential velocity and Reynolds number are increasing linearly with radius and this fact could result in the slight movement forward and the somewhat shorter discontinuity as indicated previously. However, at a fixed pitch angle and rotor speed, as a result of a varying downwash angle for an untwisted blade, a slightly different local angle of attack will exist along the blade span. For example, in the case of $\theta = 5°$ the angle of attack at 80% radius will be 2.5° and the angle of attack at 40% radius will be 1.5° using a simple hovering strip analysis. Thus, it can be seen that the changes in the pattern may be due to both velocity and angle-of-attack influences.

For increasing pitch angles, it is readily apparent that the discontinuities have moved farther forward on the airfoil where they tend to form a single spike. In the inboard regions following the discontinuity the traces tend to deviate outwardly from the circular streamlines (superimposed on traces). The reason for this outflow is not clear at this stage of the investigation.

For several test conditions the traces near the tip move inwardly relative to the reference streamlines. This action is considered to be similar to that reported by Tanner and Yaggy as being the result of the radial inflow on the upper surface induced by the tip vortex.[10] As the pitch angle is increased, the tip vortex is strengthened, thereby increasing the inward flow at the blade tip.

The traces at pitch angles of 17° and 20° at the 90% radius position disappear shortly aft of the leading edge. It appears that the boundary layer has separated from the airfoil surface. At the 80% radius position the tracer gas reflects an inward flow of the boundary layer. The most likely explanation for this inward flow lies in the nature of the spanwise pressures near the leading edge. As a result of the attached boundary layer at 70% radius and the high pitch angles, very high peak negative pressures will exist in this region. If separation has occurred at 90% radius, the pressure in this region may be greater than that in the 70% region. Thus, at 80% radius the fluid particles containing ammonia will flow inward due to this pressure differential.

A similar argument can be used to explain the apparent unrelated directions of the traces in the outboard regions of the blades at other positions and test conditions. Local regions of stalled and unstalled flow may exist simultaneously. It should be noted, however, that the effects of the pressure gradient at these high angles of attack are more significant than the influence of centrifugal force. The similarity of the inward moving traces and the outward moving traces even in the presence of a very strong centrifugal field tend to indicate the predominant influence of the spanwise pressure gradient under conditions close to stall.

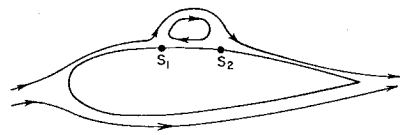

Fig. 8 Laminar separation bubble on an airfoil.

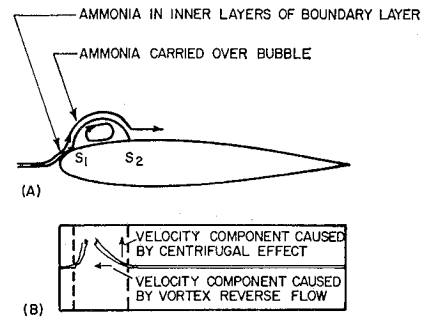

Fig. 9 Possible factors involved in the shape of the ammonia trace.

Interpretation of Results

Separation Bubble

Based upon study of the ammonia traces and the sublimation data, it was hypothesized that a standing vortex or separation bubble associated with transition occurs on the blade and causes the observed discontinuity. The occurrence of separation bubbles in two dimensions has been discussed by McCoullough and Gault and others[12,13] The pattern of a separation bubble is shown in a somewhat exaggerated drawing in Fig. 8.

If a separation bubble is present, the majority of the fluid will go over the vortex and be re-energized by gaining momentum from the freestream, by the presence of an accelerating profile caused by the bubble, and by the absence of surface friction over the length of the bubble. As a result of these three factors the flow will reattach to the surface and a turbulent boundary layer will exist.[14] The bubble causes two stagnation points, s_1 and s_2, to be present at either end of the vortex. They should not be confused with the stagnation point which occurs at the leading edge of the airfoil. It should be noted that s_1 corresponds to the initial separation point and s_2 corresponds to the point of reattachment.

The following mechanism is hypothesized for the shape of the discontinuity as seen in Fig. 3. As the ammonia vapor is injected into the boundary layer at the nose of the airfoil, it is carried aft with the boundary-layer flow. At first it forms a dark, distinct, and narrow trace. As the flow in the boundary layer with the ammonia passes the peak pressure position, it feels the adverse pressure gradient. The fluid velocity decreases and the velocity profile changes rapidly to that of a "separation profile." The forward separation point is then reached, and at this point the fluid velocity and shear stress near the surface are essentially zero. In this reduced velocity region ahead of the separation point the fluid particles containing the ammonia are subject to both the outward spanwise pressure gradient and the centrifugal force. The inner layers of the boundary layer tend to move outward under the actions of these forces. As they do so, the ammonia diffuses to the surface and leaves the forward portion of the discontinuity—an outward moving trace.

It is considered, however, that a significant portion of the ammonia in the upper layers of the boundary layer is carried by the main stream over the separation bubble in a chordwise direction. This flow then returns to the surface aft of the bubble at the reattachment point where again the chordwise fluid velocities are quite low. The local surface flow includes some forward or reverse flow towards the bubble as well as some outflow resulting from the action of either centrifugal force or spanwise pressure gradients. The combined effects of outflow and reverse flow could account for the shape of the

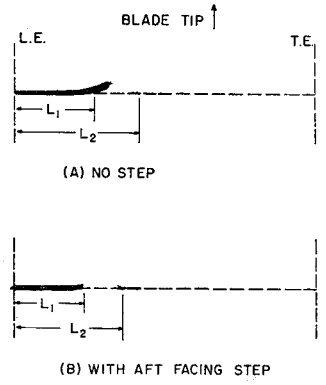

Fig. 10 Comparison of ammonia trace with and without surface step at 400 rpm and θ = 5°: A) L_1 = 21%, L_2 = 43%; B) L_1 = 20%, L_2 = 34%.

aft portion of the discontinuity. This situation is depicted in Fig. 9.

A limited amount of testing was done with boundary-layer fences on the rotor to determine if significant spanwise flow was involved in the discontinuity patterns.[15] The 1-in. fences were placed both inboard and outboard of the ammonia orifice similar to fences used in swept wings. It was found that with the fences on the blade the traces retained the same pattern as found previously.

Surface Step Studies

As the fluid approaches a separation point in the boundary layer, it decelerates and eventually leaves the airfoil. Such a separation can be avoided by changing the shape of the surface on which the separation occurs. If a cusp is put on the surface, the fluid will leave the wall tangentially with a finite velocity, and one stagnation point will be eliminated from the usual standing vortex flow pattern. A stable vortex is formed behind the cusp and this vortex prevents a laminar separation of the flow elsewhere on the blade. In this manner the position of laminar separation and transition can be controlled.

The flow over a rear facing step is an approximation to the flow over a cusp and has been studied by Tani.[16] The flow is not actually tangent when it leaves the surface and there may be several vortices, but the step has the important characteristics of the cusp. That is, only one stagnation point of the main stream, the standing vortex is present, and separation can be controlled by the step.

To study the action of the ammonia trace technique with a known separation, a step of 0.013-in. height was located at 20% chord on the blade. A comparison of the ammonia traces for 5° and 400 rpm, with and without the step being present, is shown in Fig. 10. For no step the "outward flow" trace begins gradually at 21% chord and reattaches at 43% chord. The step causes separation at 20% chord. The trace reappears at 34% chord. This indicates that the step produces a standing vortex with one reattachment stagnation point, moves the discontinuity from its original position, and alters its shape. The first part of the discontinuity is gone because no stagnation point is there to produce outward flow. A spanwise trace similar to the second half of a regular discontinuity does occur after the step. The distance that the flow is unattached was shorter, probably because the step produces a more concentrated vortex. The results of the tests with the step give strong assurance that the separation bubbles are responsible for the discontinuities seen.

Discussion of Stall

In view of the nature of the ammonia traces found and the possible existence of a standing bubble, it is considered logical to examine the nature of ordinary two dimensional stall. Low speed stall of airfoils can be classified as follows: 1) Trailing-edge stall (preceded by movement of the turbulent separation point forward from the trailing edge with increased incidence), 2) Leading-edge stall (abrupt flow separation near the leading edge generally without subsequent reattachment), and 3) Thin-airfoil stall (preceded by flow separation at the leading edge with reattachment at a point which moves progressively rearward with increasing incidence). The sequence of events preceding "leading-edge stall" are of interest since, according to Crabtree, this type of stall is associated with a "short" bubble.[17]

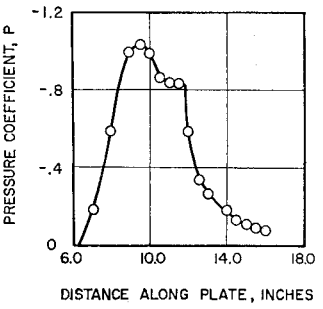

Fig. 11 Pressure distribution in the vicinity of a bubble.[13]

At a fixed freestream Reynolds number, "leading-edge stall" occurs when, as the angle of incidence is increased, the bubble gradually contracts. However, upon further increase in incidence the bubble suddenly "burst" and the flow may or may not reattach to the airfoil surface. Reattachment farther downstream will create a much larger bubble than before. Close examination of Fig. 7 indicates that as the pitch angle increases, the discontinuity moves toward the leading edge and its length tends to decrease until eventually, at the outboard location, the trace abruptly ends very near the leading edge.

Re-examination of Fig. 6, which correlates the discontinuity length with pitch angle, reveals that the decrease in discontinuity length with increased pitch is very suggestive of the events preceding leading edge stall. Recently, Crabtree[17] and Gaster[13] have given evidence that one of the controlling factors of bubble behavior is that of the pressure difference across the bubble. It is generally known that a characteristic of most separated flows is that of a constant pressure region. The pressure difference referred to by these investigators is that which would occur along the length of the bubble in the absence of the bubble. A typical pressure distribution with the presence of a bubble is shown in Fig. 11. The chordwise location of the bubble can be detected from the small step in the pressure distribution where the pressure remains approximately constant aft of the pressure peak. Direct comparison with the ammonia traces cannot be made since the airfoil section, Reynolds number, and incidence angles are not the same and no pressure data were taken. The pressure distribution across the trace discontinuity is expected to follow the same trend, however, as that seen in Fig. 11.

One of the major concerns in this study was the low Reynolds numbers attained. The maximum Reynolds number at which a discontinuity in the flow was observed was about 6.3×10^5. This is much smaller than that found on typical

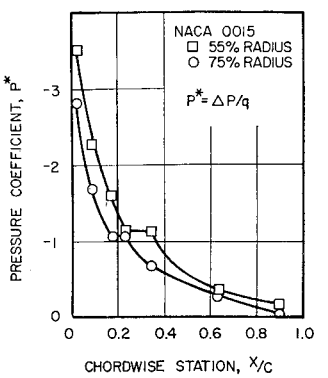

Fig. 12 Chordwise pressure distribution on a full scale helicopter rotor blade.[18]

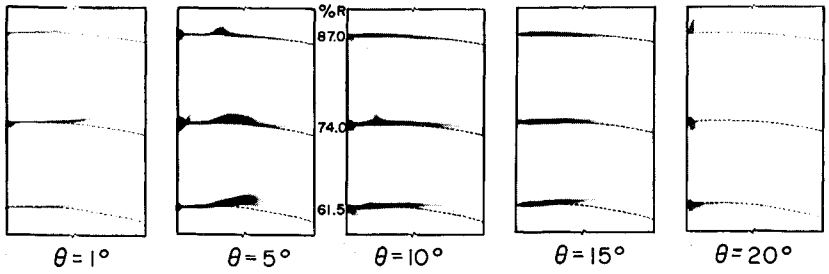

Fig. 13 Composite set of traces for 7-in. chord blade for 3 radii at 400 rpm showing effect of changing pitch angle.

full-scale helicopters near the rotor tip. However, in Fig. 12 the pressure distribution at the 55 and 75% radial positions of the HU-1A helicopter in hovering shows a pressure step pattern very similar to that in Fig. 11 (Ref. 18). The free-stream Reynolds number at the blade tip for this flight test was 5.8×10^6. It is quite improbable that laminar separation bubbles would occur at this high Reynolds number; however, the authors know of no other explanation for the pressure step exhibited by this data.

Test Results for Seven-in. Chord Blades

Hover Condition

Leading edge orifices

The series of tests of the 7-in. chord blade in the hovering condition revealed ammonia traces that were quite similar to those found with the 4-in. chord blade.

Figure 13 illustrates the effect of increasing angle of attack for the 7-in. chord blade at 400 rpm. The similarity with previous results is apparent. Comparison, however, should be made with a higher rpm condition for the 4-in. blade in order to maintain similar Reynolds numbers. The discontinuity moves forward and the width of the discontinuity becomes very short or disappears completely as the angle of attack is increased.

The influence of rotor speed at a pitch angle of 15° is shown in Fig. 14. It can be seen that distinct discontinuities occur near the leading edge at 200 rpm, whereas they are not present at 400 rpm. It would seem that at the higher speed the Reynolds number has increased sufficiently to allow transition to occur prior to the formation of the bubble. In such a case it would be expected that stall should tend to occur in a classic fashion with gradual turbulent separation progressing from the trailing edge. Examination of Fig. 13 for $\theta = 20°$ reveals, however, that the separation is complete across the entire chord. No traces are available for small step increments of θ between 15° and 20° for this airfoil, by which a better determination could be made of the nature of stall during rotation.

Network orifices

To justify the previous conclusions concerning the flow discontinuity a third rotor was tested. Orifices for the ammonia were located in the blade surface at 61.8, 68.4, 75.0, and 81.5% radius, and a number of chordwise positions. In these experiments the ammonia release time was a pulse of less than 200 ms duration, whereas in all previous tests release times were on the order of a few seconds. A typical trace obtained at 200 rpm and a pitch angle of 10° is shown in Fig. 15. The flow discontinuity is again evident. The trends of the length and chordwise position of the discontinuities with radial position are very similar to those described earlier.

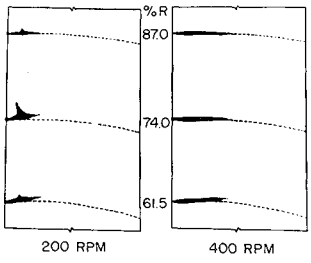

Fig. 14 Ammonia traces for 7-in. chord blade at $\theta = 15°$ showing effect of change in rpm.

In the previous tests with only a leading edge orifice the traces represented the path of the fluid elements passing over the orifice from which the ammonia was released. In the case of the network of orifices the ammonia release time is much shorter. These traces more nearly represent the instantaneous flow direction near the surface.

The pressure on the upper surface of the blade decreases with increasing radial position. As a result more ammonia will be released at 81.5 than at 61.8% radius. The more ammonia released, the longer it takes to complete the reaction with the Ozalid paper. Therefore, the outboard traces overlap and appear hazy while the inboard traces are quite clear and discrete. In the limit as the release time approaches zero the trace obtained would ideally represent the direction of the resultant surface shear stress vector.

Forward Flight Simulation

The 7-in. chord blade employing only leading edge orifices was operated in a wind tunnel to simulate forward flight rotor operations. Throughout these tests a mechanical poppet valve was used to pulse the ammonia during a preset portion of each rotor revolution. A typical set of traces is shown in Fig. 16. Advance ratios of $\mu = 0.20$, 0.25, and 0.30 were run. All test conditions utilized a mean hover lift coefficient of $C_{L_M} = 0.6$, and the flat plate area for the equivalent helicopter was adjusted for each rotor speed used.

Consider the $\mu = 0.20$ condition in Fig. 16. In general, the traces tend to follow the usual net flow in the form

$$V_r = \Omega r + V\sin\psi$$

The reference trajectory based on this equation is shown with each trace. It can readily be seen that the traces for $\psi = 0°$, 90°, and 180° are regular and indicate attached flow. No clearly delineated discontinuities appear in the traces to indicate the presence of any boundary-layer bubble. At 0°

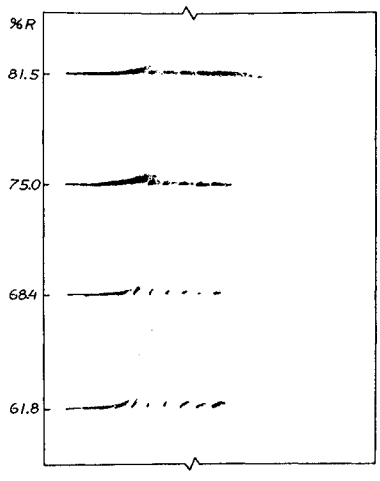

Fig. 15 Network of traces obtained at 200 rpm and $\theta = 10°$.

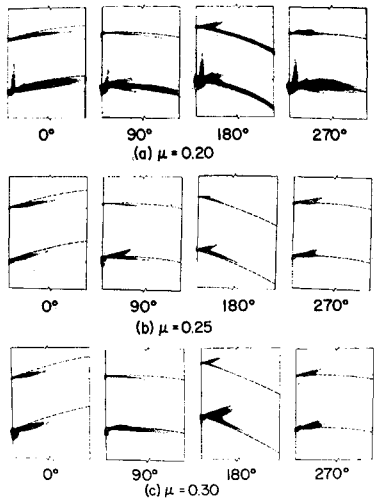

Fig. 16 Simulated forward flight traces at 500 rpm, every 90° azimuth, and radial positions of 74% and 87%.

there is some slight indication of a change in shape of the trace at about the 20% chord position of the airfoil, but no clearly defined discontinuity exists. At 90° and 180°, there are strong tendencies for the flow to turn inboard near the trailing edge of the airfoil. It is interesting to note that additional short traces emanate from the orifice at these azimuthal positions. The exact reasons for these secondary traces is not clear.

The $\psi = 270°$ traces for $\mu = 0.20$ are no longer similar to the preceding traces. Instead of being relatively continuous and well defined to the trailing edge, they exhibit the tendency to become diffuse before the midway point of the airfoil. The traces obtained at the higher advance ratios are slightly more diffuse; however, they exhibit properties similar to traces at $\mu = 0.20$.

It appears that the nature of "stall" is different in the retreating blade case from what it appears to be for the hovering case. At the Reynolds numbers used in the tests, stall in hover seems to result from a leading-edged airfoil stall. In the retreating blade case, the stall may be similar to the "soft" stall which occurs with gradual separation of the turbulent boundary layer from the trailing edge.

Conclusions

The use of the ammonia trace technique provided a valuable insight into the nature of the boundary layer of a hovering rotor. The particular discontinuities found in the traces are believed to indicate the presence of a standing "bubble." The discontinuities were found to move forward with increasing Reynolds number and to shorten with increased pitch angle. This behavior is similar to that expected for bubbles on two dimensional airfoils. Of particular interest is that such bubbles may exist over a wide range of Reynolds numbers since evidence was found which indicates the possible presence of such a bubble on a full-scale helicopter rotor in hovering. The ammonia traces at high pitch angles tend to indicate that the stall of the NACA 0015 airfoil in hovering is similar to the "sharp leading edge" type of two-dimensional stall. No indication of any separation bubbles could be found on the forward flight traces.

Although this study was directed toward helicopter rotor blade boundary-layer behavior, it is believed that the findings may be applicable to a broader range of turbomachines. For example the initial blade rows of axial flow compressors operating at high altitudes will have blade Reynolds numbers which fall in the range of Reynolds numbers covered in this work. Thus it is considered possible that laminar separation bubbles may exist in the initial compressor stages. The ammonia trace technique would also appear to be quite useful in the study of such boundary-layer action.

Further tests using the ammonia process in conjunction with other measurement techniques are needed to determine the nature of the bubbles and their effect on airfoil performance.

References

[1] Fogarty, L. E., "The Laminar Boundary Layer on a Rotating Blade," *Journal of the Aeronautical Sciences*, Vol. 18, No. 4, April 1951, pp. 247–252.

[2] Tan, H. S., "On the Laminar Boundary Layer Over a Rotating Blade," *Journal of the Aeronautical Sciences*, Vol. 20, No. 11, Nov. 1953, pp. 780–781.

[3] Liu, S. W., "The Laminar Boundary Layer on Rotating Cylinders," TN 57-298, Pts. I and II, June 1957, Air Force Office of Scientific Research.

[4] Banks, W. H. H. and Gadd, G. E., "Delaying Effect of Rotation on Laminar Separation," *AIAA Journal*, Vol. 1, No. 4, April 1963, pp. 941–942.

[5] McCroskey, W. J. and Yaggy, P. F., "Laminar Boundary Layers on Helicopter Rotors in Forward Flight," *AIAA Journal*, Vol. 6, No. 10, Oct. 1968, pp. 1919–1926.

[6] Blaser, D. A. and Velkoff, H. R., "Pressure Distribution and Angle of Attack Variation on a Helicopter Rotor Blade," *Journal of the American Helicopter Society*, Vol. 13, No. 2, April 1968, pp. 88–92.

[7] Tanner, W. H. and Beuttiker, P., "The Boundary Layer of the Hovering Rotor," *Proceedings of the CAL/USAAVLABS Symposium on Aerodynamic Problems Associated with V/STOL Aircraft*, Cornell Aeronautical Lab., Vol. III, June 1966.

[8] Ham, N. D. and Young, M. I., "Torsional Oscillation of Helicopter Blades due to Stall," *Journal of Aircraft*, Vol. 3, No. 3, May–June 1966, pp. 218–224.

[9] Johnson, J. P., "A Wall Trace, Flow Visualization Technique for Rotating Surfaces in Air," *American Society of Mechanical Engineers: Journal of Basic Engineering*, Vol. 86, No. 2, Dec. 1964, pp. 907–908.

[10] Tanner, W. H. and Yaggy, P. F., "Experimental Boundary Layer Study on Hovering Rotors," *Journal of the American Helicopter Society*, Vol. 11, No. 3, July 1966, pp. 22–37.

[11] Silverstein, A. and Becker, J. V., "Determination of Boundary Layer Transition of Three Symmetrical Airfoils in the NACA Full Scale Wind Tunnel," Rept. 637, 1939, NACA.

[12] McCoullough, G. B. and Gault, D. E., "Examples of Three Representative Types of Airfoil-section Stall at Low Speed," TN-2502, 1951, NACA.

[13] Gaster, M., "The Structure and Behaviour of Laminar Separation Bubbles," *Proceedings of the AGARD Conference on Separated Flows*, North Atlantic Treaty Organization, No. 4, Pt. 2, May 1966, pp. 813–854.

[14] Lachmann, G. V., *Boundary Layer and Flow Control*, Vol. I, Pergamon, New York, 1961, p. 173.

[15] Schlichting, H., *Boundary Layer Theory*, McGraw-Hill, New York, 1960, p. 198.

[16] Tani, I., "Experimental Investigation of Flow Separation Over a Step," *Boundary Layer Research*, edited by H. Gortler, Springer-Verlag, Berlin, 1958, pp. 377–386.

[17] Crabtree, L. F., "The Formation of Regions of Separated Flow on Wing Surfaces," R and M 3122, July 1957, Aeronautical Research Council, London.

[18] "Measurement of Dynamic Air Loads on a Full Scale Semi-rigid Rotor," TCREC TR 62-42, Dec. 1962, U.S. Army Transportation Research Command, Ft. Eustis, Va., pp. 322–323.